GEOLOGY | THE GEOLOGICAL SOCIETY OF AMERICA®

https://doi.org/10.1130/G45563.1

Manuscript received 6 September 2018
Revised manuscript received 12 April 2019
Manuscript accepted 14 April 2019

Published online 22 May 2019

A widespread olivine-rich ash deposit on Mars

Christopher H. Kremer, John F. Mustard, and Michael S. Bramble
Department of Earth, Environmental and Planetary Sciences, Brown University, 324 Brook Street, Providence, Rhode Island 02912, USA

ABSTRACT

The origins of olivine-rich rocks on Mars remain only partially constrained, with hypothesized deposition as lava flows, impact products, aeolian sand, and pyroclastic materials. These rock units' uncertain origins obscure their genetic relationships with each other and the contexts of their aqueous alteration. We synthesize geomorphic mapping and geomorphic and stratigraphic measurements with previous spectroscopic analyses to constrain the origin of the circum–Isidis Planitia olivine-rich unit, one of Mars's most widespread and mineralogically diverse olivine-rich rocks. We find that the unit most likely formed as an ash-fall deposit, with a probable origin related to volcanism in the greater Syrtis Major–Isidis Planitia region. This work corroborates hypotheses that some extensive outcrops of ancient bedrock are clastic and that a planet-wide transition from dominantly explosive to effusive volcanism may have occurred in the Hesperian. Our findings also highlight the likely diverse origins of olivine-rich martian rocks and provide key geologic context for the aqueous alteration of the unit and underlying ancient crust.

INTRODUCTION

Olivine-rich rocks have been detected in visible to infrared spectra in disparate locales on the surface of Mars (e.g., Ody et al., 2013). Multiple hypotheses exist for the origins of these rock units, including lava flows (Tornabene et al., 2008; Ody et al., 2013), magmatic intrusions (Hoefen et al., 2003), impact melt sheets (Mustard et al., 2009), impact vapor condensates (Palumbo and Head, 2018; Rogers et al., 2018), pyroclastic deposits (Bramble et al., 2017; Rogers et al., 2018), and/or epiclastic materials (Rogers et al., 2018) such as fluvial or sand sea (erg) deposits. These hypotheses have contrasting implications for the petrogenetic relationships of Mars's olivine-rich rocks with its other igneous units, the extent to which volcanism or impacts delivered mantle materials to Mars's surface, and the textural controls on their aqueous alteration.

While the origins of these rock units likely vary, we focus on the olivine-rich unit of the circum–Isidis Planitia region (Fig. 1; Figs. DR1–DR4 in the GSA Data Repository[1]), which is one of Mars's most widely exposed olivine-enriched rock units (Hoefen et al., 2003), as well as one of its most mineralogically diverse aqueously altered rocks, with spectrally detected carbonate, serpentine (Ehlmann and Mustard, 2012), and Fe-Mg phyllosilicates (Bramble et al., 2017). The circum-Isidis olivine-rich unit occurs in the Nili Fossae (Ehlmann and Mustard, 2012) and Libya Montes regions (Tornabene et al., 2008; Bishop et al., 2013), with exposures in the Mars 2020 rover (NASA Mars Exploration Program) landing site in Jezero crater (Goudge et al., 2015) and the adjacent region of Northeast Syrtis (Bramble et al., 2017).

The olivine-rich unit overlies phyllosilicate-enriched basement and underlies an olivine-poor, massive, and mafic capping rock of unknown origin (Ehlmann and Mustard, 2012). The unit is no older than the ca. 3.96 Ga Isidis-forming impact (Werner, 2008) and is locally overlain by ca. 3.6 Ga Syrtis Major lavas (Mustard et al., 2009). It is characterized by polygonal fracturing (Bramble et al., 2017), light or mottled tonality (the color scheme or range of tones) (Goudge et al., 2015), internal banding of locally alternating tonality (Hamilton and Christensen, 2005; Mustard et al., 2009; Fig. DR4), and spectral signatures suggesting olivine with a modal abundance of 10%–25% (Edwards and Ehlmann, 2015; Salvatore et al., 2018) and magnesium-rich ($Fo_{68–91}$), composition (Hamilton and Christensen, 2005). The unit apparently drapes the topographically undulating basement unit (Mustard et al., 2009).

The unit's stratigraphic position above basement rock rules out an origin as igneous intrusions (Hoefen et al., 2003). Its mantling of Jezero crater (Goudge et al., 2015), which itself postdates the Isidis basin, rules out an origin as products (Mustard et al., 2009; Palumbo and Head, 2018) from the Isidis-forming impact. Its inferred topographic draping (Mustard et al., 2009) and friability (Rogers et al., 2018) cast doubt on lava flow origins. Finally, evidence to date is equivocal that the unit was deposited as spherules from other large impacts (Edwards and Christensen, 2011), eroded and transported epiclastic sediment, or air-fall pyroclasts (Rogers et al., 2018). Based on previous interpretations of abundant pyroclastic rocks on Mars (e.g., Kerber et al., 2012; Bandfield et al., 2013) and in situ observations of martian pyroclastic rocks (Squyres et al., 2007), including olivine-rich ash (Ruff et al., 2014), we undertake a detailed geomorphic and stratigraphic study to test whether the unit may have been deposited as volcanic ash.

We assess the unit's origin using regional 1:50,000-scale geomorphic mapping and detailed measurements and observations of its thickness, topographic distribution, internal stratigraphy, and draping geometries. We compare our results with previous spectroscopic analysis and the expected characteristics of ash, erg, lava, and non-Isidis impact products in physical and conceptual models, finding that the unit is most likely a pyroclastic rock with a probable source within the greater Syrtis-Isidis region.

MAPPING AND MEASUREMENTS

We mapped the olivine-rich unit (Fig. 1; Figs. DR1–DR4) using (1) spectral signatures of olivine in data from the Mars Reconnaissance Orbiter (MRO) Compact Reconnaissance Imaging Spectrometer for Mars (CRISM) (Murchie et al., 2007), (2) geomorphic features characteristic of the unit in orbital imagery from the MRO High Resolution Imaging Science

[1]GSA Data Repository item 2019249, description of methodology, Figures DR1–DR9, and Tables DR1–DR6, is available online at http://www.geosociety.org/datarepository/2019/, or on request from editing@geosociety.org.

CITATION: Kremer, C.H., Mustard, J.F., and Bramble, M.S., 2019, A widespread olivine-rich ash deposit on Mars: Geology, v. 47, p. 677–681, https://doi.org/10.1130/G45563.1

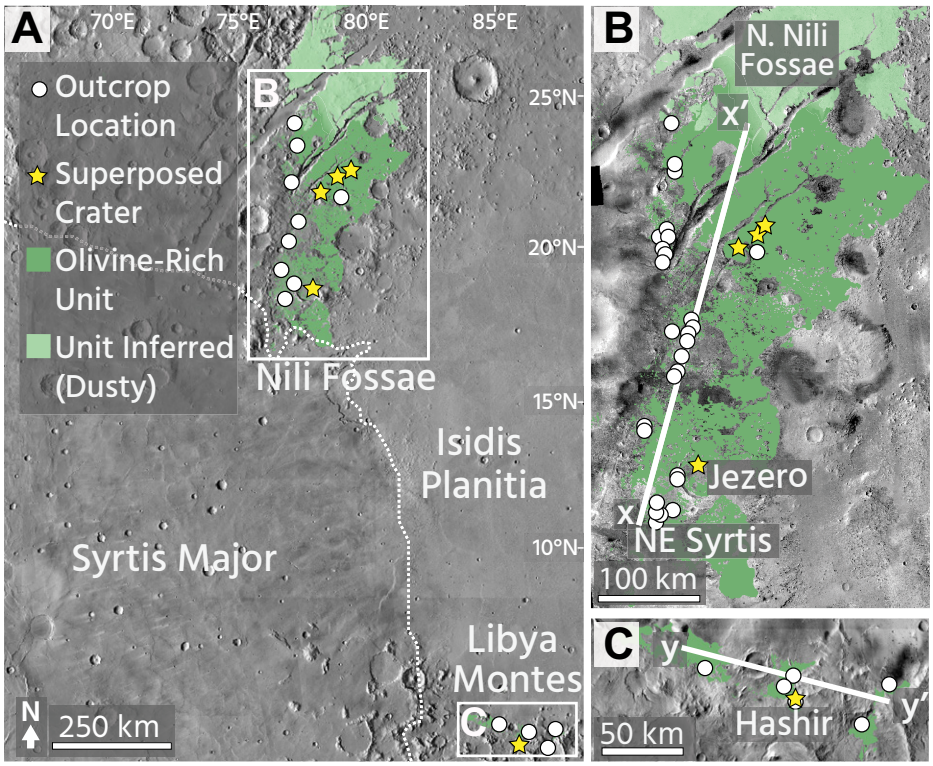

Figure 1. A: Map of circum–Isidis Planitia (Mars) olivine-rich unit exposures (darker green) and inferred extent (lighter green) overlaid on Mars Reconnaissance Orbiter Context Camera (CTX) mosaic (Dickson et al., 2018). For criteria used to map inferred extent of the unit in dust-covered northern Nili Fossae, refer to Item DR1 in the Data Repository (see footnote 1). Syrtis Major's extent is shown with dotted line. B: Exposures and inferred extent of unit in Nili Fossae. C: Exposures of unit in Libya Montes. Lines x-x′ and y-y′ (Fig. 4) are labeled in B and C. Post-Isidis craters superposed by the unit, schematic locations of ~120 measured outcrops, and locales named in text are labeled.

Experiment (HiRISE) (McEwen et al., 2007) and imagery mosaics (Dickson et al., 2018) from the MRO Context Camera (CTX) (Malin et al., 2007), and (3) previous spectroscopic and geomorphic maps of the unit (Hamilton and Christensen, 2005; Tornabene et al., 2008; Goudge et al., 2015; Bramble, et al., 2017). We used the NASA Ames Stereo Pipeline software (Moratto et al., 2010; https://ti.arc.nasa.gov/tech/asr/groups/intelligent-robotics/ngt/stereo/) to create digital elevation models (DEMs) from HiRISE and CTX imagery to assess the unit's stratigraphy, banding orientation (Fig. 2), topographic distribution (Fig. 3), and thickness (Fig. 4). We also used elevation data from the High Resolution Stereo Camera (HRSC) on Mars Express (Neukum et al., 2004) and the Mars Orbiter Laser Altimeter on Mars Global Surveyor (Smith et al., 2001) to assess topographic distribution.

We estimated outcrop thicknesses by measuring the total elevation change between the unit's highest and lowest topographic exposures. We measured outcrops showing contacts with both the overlying cap rock and underlying basement unit (complete stratigraphic sections) or with just one unit (partial sections). Dips of the unit's banding and contacts with the basement and cap rock were estimated by extracting elevations from DEMs and fitting a plane to the non-collinear point cloud for each band or contact. We calculated the average thicknesses of bands, which are exceptionally well resolved because of their alternating tonality, by dividing the thickness of each outcrop by the number of bands observed per outcrop. For detailed methodologies, see Item DR1 in the Data Repository.

RESULTS

Banding and Contact Orientations

Internal bands are approximately parallel with each other and with the unit's basal and top contacts in ~40 measured outcrops (Fig. 2). Dips vary more for each outcrop in Libya Montes, where basement topography is more rugged than in Nili Fossae. Parallelism of internal banding and its co-occurrence with "stair-step" or ledge-forming morphologies in DEMs indicate that it is layering (Fig. 2; Fig. DR5). Parallelism between the olivine-rich unit's bedding and its contact with the basement rock confirms that the unit drapes underlying topography. Parallelism of the unit's bedding and its contact with the cap rock suggests that the unit experienced limited erosion before the cap rock's emplacement.

Banding is almost exclusively concentric in plan view and is continuous and parallel in cross-section, exhibiting no internal truncations at the decimeter to decameter scales, consistent with plane bedding (Fig. 2; Figs. DR6–DR7). Elongate ridges composed of the unit, previously interpreted locally as flow features (Hamilton and Christensen, 2005), have been reinterpreted as yardangs (Bishop et al., 2013; Day and Dorn, 2019; see also Fig. DR8).

Topographic Distribution

The unit's exposed and inferred occurrences span ~4000 m of topographic elevation across its total outcrop extent in the circum-Isidis region, which we estimate at ~70,000 km^2 (Fig. 3). The unit drapes much of Jezero crater's rim, rising ~100 to ~700 m above the surrounding terrain (Fig. 3; Fig. DR9). The unit drapes nearly the entirety of three crater-like structures in Nili Fossae, rising ~300 to ~600 m above the surrounding terrain (Fig. DR9). The unit is also exposed on the lower rim of Hashir crater, ~35 m above its top contact with the cap rock on the crater floor. The fracturing and banding in these outcrops imply that the unit is in place.

Thickness and Stratigraphy

The thicknesses of ~120 outcrops of the olivine-rich unit were measured with HiRISE and CTX DEMs, and complete stratigraphic sections of the unit in Nili Fossae range from ~2 to ~23 m in thickness (Fig. 4). Thicknesses of partial sections range up to ~104 m in Libya Montes, where two complete sections are ~48 and ~68 m thick. The unit's overall average thickness is ~10 m, up to an order of magnitude thinner than previous estimates (Mustard et al., 2009). In Nili Fossae, the unit's thickness crudely decreases with distance from Syrtis Major and is generally thinner than in more Syrtis-proximal Libya Montes, where the paucity of complete stratigraphic sections implies that erosion has erased depositional thickness trends. Resolvable band thicknesses range from ~0.2 to ~2.0 m (average of ~0.7 m; Fig. 4), with suggestive evidence for sub-decimeter banding (Fig. 4D; Fig. DR6). Individual bands are continuous over distances of as much as ~3 km (Fig. DR6).

DISCUSSION

Here we synthesize our results with previous observations and spectroscopic analyses of the olivine-rich unit, finding that our results are most consistent with its emplacement as ash-fall deposits.

Superposition of in-place olivine-rich outcrops on the hundreds-of-meters-tall rims of at least five craters (Fig. 2; Fig. DR9), which exhibit no rim-piercing dikes, rules out the emplacement of the unit as lava flows. The unit spans ~4000 m of elevation and does not

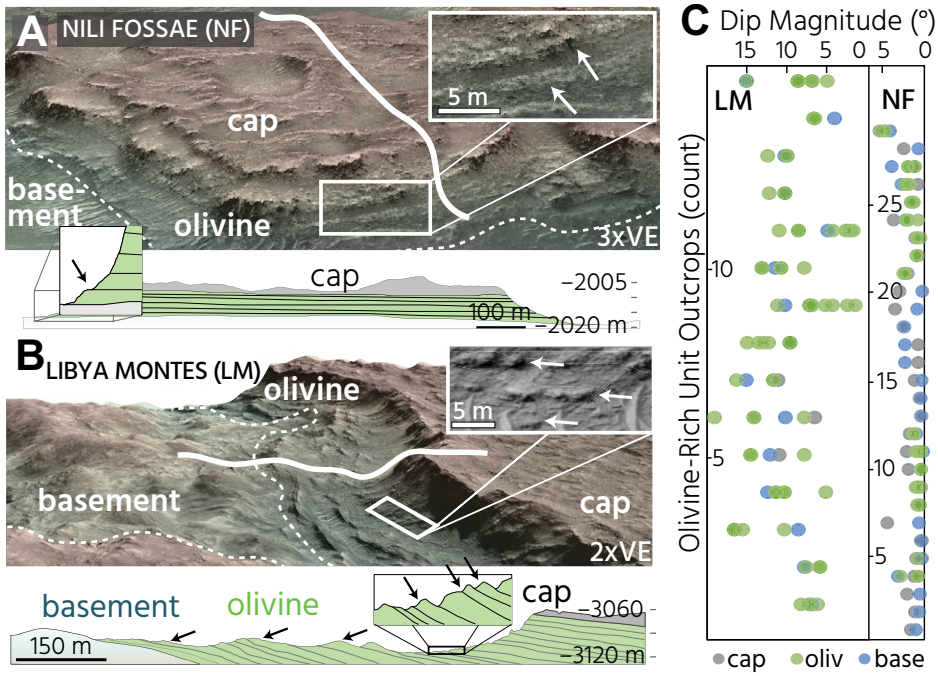

Figure 2. A: Mesa (17.9°N, 77.1°E) in Northeast Syrtis in Nili Fossae (Mars) showing parallelism of layers in olivine-rich unit and contacts with basement and capping units. B: Mesa in Hashir crater (3.2°N, 85.0°E) in Libya Montes showing parallelism of olivine-rich unit layers and contacts. Extracted cross-section locations in A and B are shown as white lines on digital elevation models (DEMs), where red and green shading on DEMs denote relative elevation (red is higher, green is lower). "Stair-step" bedding is marked with white and black arrows. VE—vertical exaggeration. C: Measured dips of vertically resolvable bands in olivine-rich unit (green) and contacts between olivine-rich unit and cap rock (gray) and basement (blue), where each row is single outcrop, with outcrops arranged along lines x-x′ and y-y′ from Figure 1. Errors are generally small (Table DR4 [see footnote 1]). Imagery identification details and more examples are shown in Figures DR5–DR6.

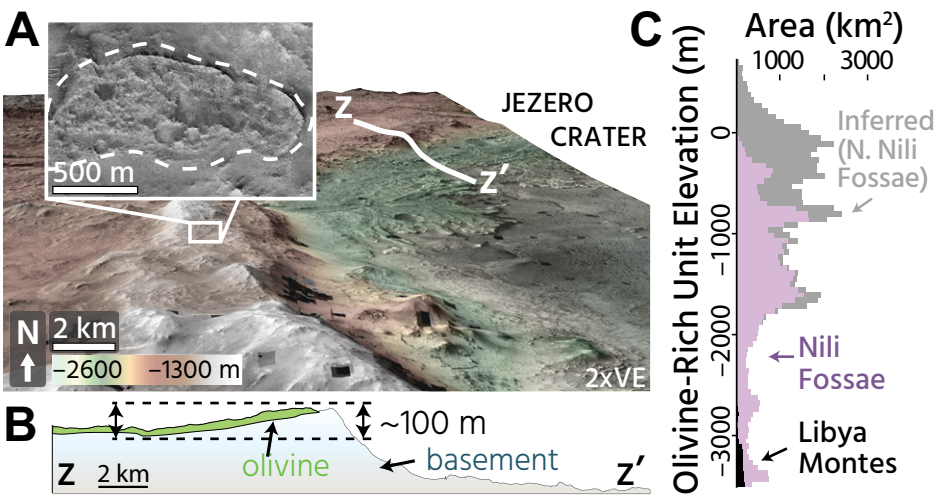

Figure 3. A: Olivine-rich unit superposing rim of Jezero crater (Mars; 18.4°N, 77.7°E) in digital elevation model. Inset shows olivine-rich mesa (outlined) ~675 m above surrounding terrain, similar in morphology to in-place olivine-rich mesas elsewhere. Red to green shading denotes elevation, ranging from –1022 m (floor of Jezero) to –1300 m (rim of Jezero, foreground). B: Unit's measured topographic distribution along line of section z-z′ in A, inferred from morphology and spectroscopy. Unit's minimum elevation above surrounding terrain is noted. C: Unit's topographic range in circum-Isidis region, derived from Mars Orbiter Laser Altimeter on Mars Global Surveyor, relative to Mars datum and binned by area. Libya Montes area (black) is small. Imagery identification details and more examples are shown in Figure DR9 (see footnote 1).

flow along topographic lows (Tornabene et al., 2008), but instead drapes tall, steep structures (Fig. 2; Fig. DR9). Flow features are absent across 70,000 km² of outcrop (Fig. DR8). Ubiquitous decimeter-scale or thinner layering within the unit is at least two orders of magnitude thinner than the decameter thicknesses modeled for ultramafic flood lavas on Mars (Keszthelyi et al., 2000), and thinner and more continuous than typical terrestrial komatiite flows (Arndt, 1986).

The unit's wide thickness range and thin internal layering (Fig. 4) differ markedly from those of globally distributed spherule deposits on Earth, which lack internal layering and exhibit thicknesses varying by less than one order of magnitude (Simonson and Glass, 2004). Proposed correlative rock units of hypothesized impact origin elsewhere on Mars lack the olivine-rich unit's distinctive banding and fracturing (Edwards and Christensen, 2011), suggesting against an impact origin, related to Isidis or otherwise.

The unit's spectroscopically inferred grain size of ~1 mm (Edwards and Ehlmann, 2015) significantly exceeds the dominant grain sizes observed in martian aeolian sands (Item DR2). Besides the unit itself, Fo-rich olivine is rare in the circum-Isidis region, meaning that either a proximal bedrock sediment source was completely eroded or buried, or the unit's $Fo_{68–91}$ olivine sand was transported and mechanically eroded over many hundreds of kilometers (Ody et al., 2013), further inconsistent with the unit's inferred grain size. Wind-blown sediments are unlikely to have the observed conformable contacts with overlying rock, and erg deposits would generally fill, not drape, topographic lows (Livingstone and Warren, 1996). A widespread erg deposit would likely exhibit cross-bedding at the decimeter to decameter scales, which is absent over the unit's ~70,000 km² extent (Fig. 2), but this might instead reflect low climb angles of migrating dunes.

Meanwhile, distal ash-fall deposits commonly exhibit a wide topographic range, draping of underlying topography, and highly continuous, decimeter- to meter-scale planar bedding of alternating tonality (e.g., Houghton and Carey, 2015), which are all evident in the olivine-rich unit (Figs. 2–4). Friable, readily deflated rocks should have moderately high thermal inertia (TI) values because they are less likely than lavas to accumulate thick, low-TI regolith (Rogers et al., 2018). Therefore, moderate TI values (Bramble et al., 2017), the presence of yardangs, and sparse regolith cover similarly indicate that friable clastic rocks compose the olivine-rich unit (Rogers et al., 2018). The unit's inferred mineralogy (10%–25% olivine) and grain size (~1 mm) are similar to those of olivine-rich pyroclastic rocks observed in situ at Columbia Hills (Ruff et al., 2014).

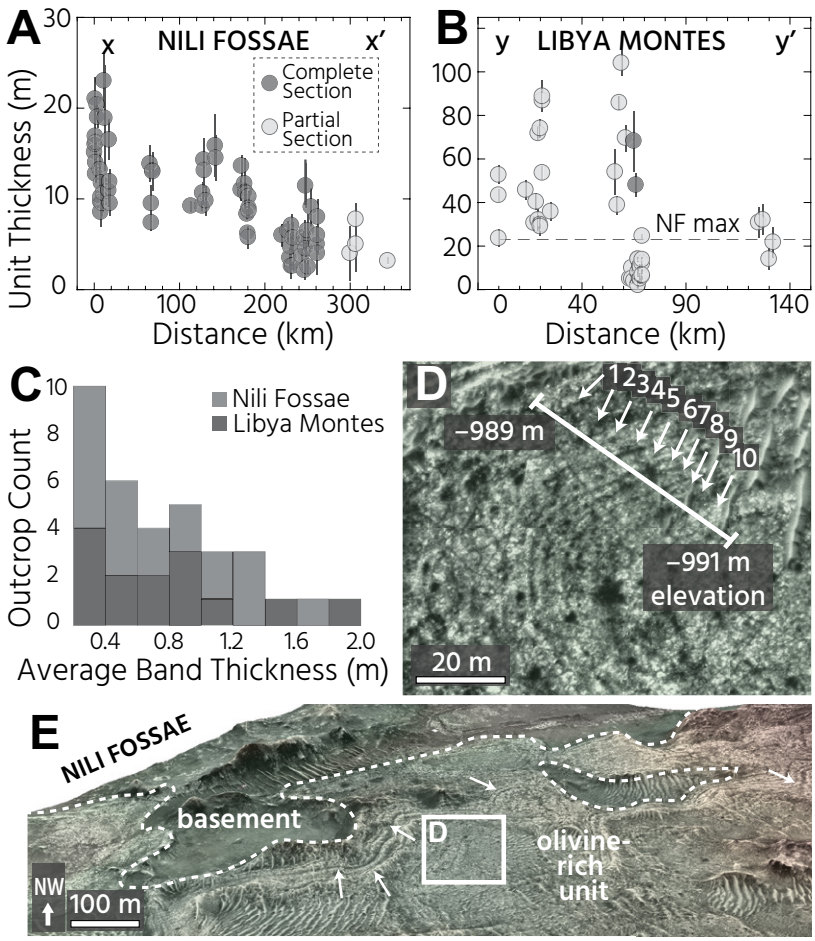

Figure 4. A: Thicknesses of partial (light gray) and complete (dark gray) olivine-rich unit stratigraphic sections in Nili Fossae (Mars). B: Thicknesses of unit in Libya Montes. Maximum thickness in Nili Fossae (NF) is shown as dashed line. Locations of lines x-x′ and y-y′ in A and B are given in Figure 1, parallel to long axes of outcrop distribution in Nili Fossae and Libya Montes. C: Average internal band thicknesses per olivine-rich unit outcrop. D: Decimeter-scale bands in an exposure of the unit (20.9°N, 77.6°E) in Nili Fossae with bands numbered and traversed topographic range labeled. E: Topographic context of D on gentle hill slope in digital elevation model. Arrows indicate ledge-forming bands. Red to green shading denotes relative elevation in D and E. Imagery identification details and more examples are shown in Figs. DR5H and DR6 (see footnote 1).

Models of explosive eruptions on Mars imply that >0.5-mm-diameter ash would have been capable of traveling hundreds of kilometers from vents in the greater Syrtis-Isidis region under a thicker early martian atmosphere (Wilson and Head, 2007), but not thousands of kilometers to the greater Syrtis-Isidis region from volcanoes elsewhere on Mars (Kerber et al., 2012). Thickness data leave the exact provenance ambiguous, and source vents have potentially been degraded by ~3.6 b.y. of erosion or covered by the extensive lavas that emanated from Syrtis Major and filled Isidis Planitia (Fig. 1), consistent with recent discoveries of poorly exposed volcanoes elsewhere on Mars (Xiao et al., 2012; Michalski and Bleacher, 2013). The olivine-rich unit's circum-Isidis distribution has been hypothesized to imply that crustal thinning by the Isidis-forming impact facilitated regional volcanism (Tornabene et al., 2008). However, this relationship remains ambiguous because younger volcanic deposits (Tornabene et al., 2008) and dust may obscure the unit's original extent.

CONCLUSION AND IMPLICATIONS

The olivine-rich unit's characteristics collectively indicate that it most likely was emplaced as an ash-fall deposit from possible source vents in the greater Syrtis-Isidis region, some of which may have been subsequently covered or eroded. The clastic nature of widespread olivine-rich rock in the circum-Isidis region strengthens arguments that significant regions of Mars's ancient olivine-rich bedrock may be clastic deposits rather than lavas (Rogers et al., 2018). The unit's superposition by ca. 3.6 Ga Syrtis Major lavas agrees with a hypothesized planet-wide transition in the Hesperian from dominantly explosive to effusive volcanism (Robbins et al., 2011; Bandfield et al., 2013), and this study provides criteria to test this hypothesis elsewhere. In situ observations of similarly olivine-rich pyroclastic rocks at Columbia Hills (Ruff et al., 2014) may also indicate a more common process of olivine-rich pyroclastic explosive volcanism on early Mars. The circum-Isidis unit's olivine abundance suggests that, like some of Mars's other olivine-enriched volcanic rocks (Monders et al., 2007), it might have been derived from primitive mantle melts. However, the olivine-rich unit's relationship with the geochemical evolution of Mars volcanism is unclear (Baratoux et al., 2011).

The high permeability and porosity of some pyroclastic deposits (Gonnermann and Manga, 2007) may account for the circum-Isidis unit's higher degree of aqueous alteration than minimally altered olivine-rich rocks on Mars of probable impact-melt origin (Ody et al., 2013). Low emplacement temperatures (<0 °C) hypothesized for distal ash (Wilson and Head, 2007) imply that the olivine-rich unit would not have supplied sufficient heat for contact metamorphism of basement rocks (Viviano et al., 2013). The olivine-rich unit's distinctive mineralogy and potential record of global volcanic transitions make it a crucial target for future in situ exploration.

ACKNOWLEDGMENTS

A Chancellor Tisch Fellowship (Brown University, Rhode Island, USA) to Kremer supported this work. We thank Steve Ruff, Josh Bandfield, Deanne Rogers, and two anonymous reviewers for very helpful reviews; the NASA Mars Reconnaissance Orbiter and Planetary Data System teams for producing and sharing data; and Jay Dickson for access to MRO Context Camera mosaics.

REFERENCES CITED

Arndt, N.T., 1986, Differentiation of komatiite flows: Journal of Petrology, v. 27, p. 279–301, https://doi.org/10.1093/petrology/27.2.279.

Bandfield, J.L., Edwards, C.S., Montgomery, D.R., and Brand, B.D., 2013, The dual nature of the martian crust: Young lavas and old clastic materials: Icarus, v. 222, p. 188–199, https://doi.org/10.1016/j.icarus.2012.10.023.

Baratoux, D., Toplis, M.J., Monnereau, M., and Gasnault, O., 2011, Thermal history of Mars inferred from orbital geochemistry of volcanic provinces: Nature, v. 475, p. 254–254, https://doi.org/10.1038/nature10220.

Bishop, J.L., et al., 2013, Mineralogy and morphology of geologic units at Libya Montes, Mars: Ancient aqueously derived outcrops, mafic flows, fluvial features, and impacts: Journal of Geophysical Research: Planets, v. 118, p. 487–513, https://doi.org/10.1029/2012JE004151.

Bramble, M.S., Mustard, J.F., and Salvatore, M.R., 2017, The geological history of Northeast Syrtis Major, Mars: Icarus, v. 293, p. 66–93, https://doi.org/10.1016/j.icarus.2017.03.030.

Day, M., and Dorn, T., 2019, Wind in Jezero crater, Mars: Geophysical Research Letters, v. 46, p. 3099–3107, https://doi.org/10.1029/2019GL082218.

Dickson, J.L., Kerber, L., Fassett, C.I., and Ehlmann, B.L., 2018, A global, blended CTX mosaic of Mars with vectorized seam mapping: A new mosaicking pipeline using principles of non-destructive image editing: Abstract 2840 presented at the 49th Lunar and Planetary Science Conference, The Woodlands, Texas, 19–23 March.

Edwards, C.S., and Christensen, P.R., 2011, Evidence for a widespread olivine-rich layer on Mars: Identification of a global impact ejecta deposit?: Abstract 2560 presented at the 42nd Lunar and Planetary Science Conference, The Woodlands, Texas, 7–11 March.

Edwards, C.S., and Ehlmann, B.L., 2015, Carbon sequestration on Mars: Geology, v. 43, p. 863–866, https://doi.org/10.1130/G36983.1.

Ehlmann, B.L., and Mustard, J.F., 2012, An in-situ record of major environmental transitions on early Mars at Northeast Syrtis Major: Geophysical Research Letters, v. 39, L11202, https://doi.org/10.1029/2012GL051594.

Gonnermann, H.M., and Manga, M., 2007, The fluid mechanics inside a volcano: Annual Review of Fluid Mechanics, v. 39, p. 321–356, https://doi.org/10.1146/annurev.fluid.39.050905.110207.

Goudge, T.A., Mustard, J.F., Head, J.W., Fassett, C.I., and Wiseman, S.M., 2015, Assessing the mineralogy of the watershed and fan deposits of the Jezero crater paleolake system, Mars: Journal of Geophysical Research: Planets, v. 120, p. 775–808, https://doi.org/10.1002/2014JE004782.

Hamilton, V.E., and Christensen, P.R., 2005, Evidence for extensive, olivine-rich bedrock on Mars: Geology, v. 33, p. 433–436, https://doi.org/10.1130/G21258.1.

Hoefen, T.M., Clark, R.N., Bandfield, J.L., Smith, M.D., Pearl, J.C., and Christensen, P.R., 2003, Discovery of olivine in the Nili Fossae region of Mars: Science, v. 302, p. 627–630, https://doi.org/10.1126/science.1089647.

Houghton, B., and Carey, R.J., 2015, Pyroclastic fall deposits, *in* Sigurdsson, H., et al., eds., Encyclopedia of Volcanoes (second edition): London, Academic Press, p. 599–616, https://doi.org/10.1016/B978-0-12-385938-9.00034-1.

Kerber, L., Head, J.W., Madeleine, J.-B., Forget, F., and Wilson, L., 2012, The dispersal of pyroclasts from ancient explosive volcanoes on Mars: Implications for the friable layered deposits: Icarus, v. 219, p. 358–381, https://doi.org/10.1016/j.icarus.2012.03.016.

Keszthelyi, L., McEwen, A.S., and Thordarson, T., 2000, Terrestrial analogs and thermal models for Martian flood lavas: Journal of Geophysical Research, v. 105, p. 15,027–15,049, https://doi.org/10.1029/1999JE001191.

Livingstone, I., and Warren, A., 1996, Aeolian Geomorphology: An Introduction: Harlow, UK, Addison Wesley Longman, 211 p.

Malin, M.C., et al., 2007, Context Camera investigation on board the Mars Reconnaissance Orbiter: Journal of Geophysical Research, v. 112, E05S04, https://doi.org/10.1029/2006JE002808.

McEwen, A.S., et al., 2007, Mars Reconnaissance Orbiter's High Resolution Imaging Science Experiment (HiRISE): Journal of Geophysical Research: Planets, v. 112, E05S02, https://doi.org/10.1029/2005JE002605.

Michalski, J.R., and Bleacher, J.E., 2013, Supervolcanoes within an ancient volcanic province in Arabia Terra, Mars: Nature, v. 502, p. 47–52, https://doi.org/10.1038/nature12482.

Monders, A.G., Médard, E., and Grove, T.L., 2007, Phase equilibrium investigations of the Adirondack class basalts from the Gusev plains, Gusev crater, Mars: Meteoritics & Planetary Science, v. 42, p. 131–148, https://doi.org/10.1111/j.1945-5100.2007.tb00222.x.

Moratto, Z.M., Broxton, M.J., Beyer, R.A., Lundy, M., and Husmann, K., 2010, Ames Stereo Pipeline, NASA's open source automated stereogrammetry software: Abstract 2364 presented at the 41st Lunar and Planetary Science Conference, The Woodlands, Texas, 1–5 March.

Murchie, S., et al., 2007, Compact Reconnaissance Imaging Spectrometer for Mars (CRISM) on Mars Reconnaissance Orbiter (MRO): Journal of Geophysical Research, v. 112, E05S03, https://doi.org/10.1029/2006JE002682.

Mustard, J.F., Ehlmann, B.L., Murchie, S.L., Poulet, F., Mangold, N., Head, J.W., Bibring, J.-P., and Roach, L.H., 2009, Composition, morphology, and stratigraphy of Noachian crust around the Isidis basin: Journal of Geophysical Research, v. 114, E00D12, https://doi.org/10.1029/2009JE003349.

Neukum, G., Jaumann, R., and the HRSC Co-Investigator and Experiment Team, 2004, HRSC: The High Resolution Stereo Camera of Mars Express, *in* Wilson, A., ed., Mars Express: The Scientific Payload: European Space Agency Publication SP-1240, p. 17–35.

Ody, A., Poulet, F., Bibring, J.-P., Loizeau, D., Carter, J., Gondet, B., and Langevin, Y., 2013, Global investigation of olivine on Mars: Insights into crust and mantle compositions: Journal of Geophysical Research: Planets, v. 118, p. 234–262, https://doi.org/10.1029/2012JE004149.

Palumbo, A.M., and Head, J.W., 2018, Impact cratering as a cause of climate change, surface alteration, and resurfacing during the early history of Mars: Meteoritics & Planetary Science, v. 53, p. 687–725, https://doi.org/10.1111/maps.13001.

Robbins, S.J., Di Achille, G., and Hynek, B.M., 2011, The volcanic history of Mars: High-resolution crater-based studies of the calderas of 20 volcanoes: Icarus, v. 211, p. 1179–1203, https://doi.org/10.1016/j.icarus.2010.11.012.

Rogers, A.D., Warner, N.H., Golombek, M.P., Head, J.W., III, and Cowart, J.C., 2018, Areally extensive surface bedrock exposures on Mars: Many are clastic rocks, not lavas: Geophysical Research Letters, v. 45, p. 1767–1777, https://doi.org/10.1002/2018GL077030.

Ruff, S.W., Niles, P.B., Alfano, F., and Clarke, A.B., 2014, Evidence for a Noachian-aged ephemeral lake in Gusev crater, Mars: Geology, v. 42, p. 359–362, https://doi.org/10.1130/G35508.1.

Salvatore, M.R., Goudge, T.A., Bramble, M.S., Edwards, C.S., Bandfield, J.L., Amador, E.S., Mustard, J.F., and Christensen, P.R., 2018, Bulk mineralogy of the NE Syrtis and Jezero crater regions of Mars derived through thermal infrared spectral analyses: Icarus, v. 301, p. 76–96, https://doi.org/10.1016/j.icarus.2017.09.019.

Simonson, B.M., and Glass, B.P., 2004, Spherule layers: Records of ancient impacts: Annual Review of Earth and Planetary Sciences, v. 32, p. 329–361, https://doi.org/10.1146/annurev.earth.32.101802.120458.

Smith, D.E., et al., 2001, Orbiter Laser Altimeter: Experiment summary after the first year of global mapping of Mars: Journal of Geophysical Research, v. 106, p. 23,689–23,722, https://doi.org/10.1029/2000JE001364.

Squyres, S.W., et al., 2007, Pyroclastic activity at home plate in Gusev Crater, Mars: Science, v. 316, p. 738–742, https://doi.org/10.1126/science.1139045.

Tornabene, L.L., Moersch, J.E., McSween, H.Y., Hamilton, V.E., Piatek, J.L., and Christensen, P.R., 2008, Surface and crater-exposed lithologic units of the Isidis Basin as mapped by coanalysis of THEMIS and TES derived data products: Journal of Geophysical Research, v. 113, E10001, https://doi.org/10.1029/2007JE002988.

Viviano, C.E., Moersch, J.E., and McSween, H.Y., 2013, Implications for early hydrothermal environments on Mars through the spectral evidence for carbonation and chloritization reactions in the Nili Fossae region: Journal of Geophysical Research: Planets, v. 118, p. 1858–1872, https://doi.org/10.1002/jgre.20141.

Werner, S.C., 2008, The early martian evolution—Constraints from basin formation ages: Icarus, v. 195, p. 45–60, https://doi.org/10.1016/j.icarus.2007.12.008.

Wilson, L., and Head, J.W., 2007, Explosive volcanic eruptions on Mars: Tephra and accretionary lapilli formation, dispersal and recognition in the geologic record: Journal of Volcanology and Geothermal Research, v. 163, p. 83–97, https://doi.org/10.1016/j.jvolgeores.2007.03.007.

Xiao, L., Huang, J., Christensen, P.R., Greeley, R., Williams, D.A., Zhao, J., and He, Q., 2012, Ancient volcanism and its implication for thermal evolution of Mars: Earth and Planetary Science Letters, v. 323, p. 9–18, https://doi.org/10.1016/j.epsl.2012.01.027.

Printed in USA